INTERNATIONAL JOURNAL OF CLIMATOLOGY
Int. J. Climatol. **27**: 157–167 (2007)
Published online 8 September 2006 in Wiley InterScience
(www.interscience.wiley.com) DOI: 10.1002/joc.1380

RMetS
ROYAL METEOROLOGICAL SOCIETY

ENSO and the South China Sea summer monsoon onset

Wen Zhou† and Johnny C. L. Chan*
Laboratory for Atmospheric Research, Department of Physics and Materials Science, City University of Hong Kong, Hong Kong, China

Abstract:

This paper investigates the relationship between the onset date of the South China Sea summer monsoon (SCSSM) and the El Niño/Southern Oscillation (ENSO). The monsoon onset date (MOD) is defined on the basis of the switch of the 850-hPa zonal winds over the South China Sea (SCS) from easterly to westerly for two consecutive pentads. The ENSO signal is represented by the ocean heat content (OHC), which is proportional to the depth of the 20 °C isotherm.

It is found that, in years associated with a warm (cold) ENSO event or the year after, the monsoon tends to have a late (an early) onset and the intensity of the SCSSM also tends to be weaker (stronger). During a 2-year period prior to the onset, anomalies of OHC have an obvious eastward propagation. The 850-hPa flow east of the Philippines, specifically the strength of the subtropical high, is also found to be critical in determining the MOD. The link between these two results appears to be the propagation of cold (warm) subsurface water into the western North Pacific (WNP), which strengthens (weakens) the subtropical high, and hence a late (an early) SCSSM onset. Copyright © 2006 Royal Meteorological Society

KEY WORDS ENSO cycle; South China Sea monsoon onset; ocean heat content

Received 12 June 2005; Revised 11 January 2006; Accepted 30 May 2006

1. INTRODUCTION

The relationship between the Asian monsoon and the El Niño/Southern Oscillation (ENSO) has been studied extensively (e.g. Angell, 1981; Rasmusson and Carpenter, 1983; Huang and Sun, 1992; Webster and Yang, 1992; Wang *et al*., 2000a,b; Chang *et al*., 2000; Kinter *et al*., 2002). Huang and Sun (1992) found that the interannual and intraseasonal variations of climate in East Asia and the general circulation over the Northern Hemisphere are closely linked to convective activities in the tropical western Pacific. Nitta and Hu (1996) obtained positive correlations between the rainfall–temperature coupled patterns and sea-surface temperature anomalies (SSTA) in the North Pacific and the tropical western Pacific.

Many researchers have attempted to establish a relationship between ENSO and the Indian summer monsoon (e.g., Ju and Slingo, 1995). However, how ENSO affects the South China Sea summer monsoon (SCSSM) and the associated East Asian summer monsoon (EASM) is relatively less explored except for a few studies. For example, Wang *et al*. (2000a) have found that ENSO events can affect East Asia climate through a Pacific–East Asia (PEA) teleconnection, with an anomalous anticyclone east of the Philippines during ENSO events. Zhang *et al*. (1996) emphasized the effects of El Niño (EN) events on the EASM through the variation of convective activity over the equatorial western Pacific. Oort and Yienger (1996) found that during the La Niña (LN), the local Hadley circulation is suppressed (enhanced) over the western tropical Pacific and enhanced (suppressed) over the eastern tropical Pacific. As the western Pacific subtropical high (WPSH) is closely related to SCSSM, it seems that ENSO might affect SCSSM through modification of the Hadley circulation and the WPSH.

Further, the SCSSM onset indicates the beginning of the EASM (Wang *et al*., 2004). An early or late SCSSM onset could affect the precipitation pattern of the EASM to some extent. Although a consensus on the domain and the definition of the SCSSM onset has yet to be reached (So and Chan, 1997; Wang and Wu, 1997; Ding and Li, 1999; Li and Mu, 1999), a general conclusion from these studies is that such an onset is associated with a switch of the zonal winds over the South China Sea (SCS) from easterly to westerly, and a concomitant increase in convective activity. The onset of the EASM is often signified by an abrupt increase in precipitation (Tao and Chen, 1987). The SCSSM onset has therefore been considered as the beginning of the East Asian subtropical summer monsoon evolution (Tao and Chen, 1987; Lau and Yang, 1997).

This study explores the possible impact of the tropical Pacific SST anomalies on the SCSSM onset. The SCS is located at the junction of three major summer monsoon components: the Indian summer monsoon, the western North Pacific (WNP) summer monsoon, and the East Asian subtropical monsoon (Wang and Wu, 1997), and

* Correspondence to: Johnny C. L. Chan, Department of Physics and Materials Science, City University of Hong Kong, Tat Chee Ave., Kowloon, Hong Kong, China. E-mail: Johnny.Chan@cityu.edu.hk
† Current affiliation: LASG, Institute of Atmospheric Physics, Chinese Academy of Sciences, Beijing, China

also in the western part of the Pacific Ocean. Thus, a study of the SCSSM onset has an important contribution towards understanding the Asian monsoon variability, and activities on the western or central Pacific should have significant effects on the SCSSM system.

In Section 2, the data used in this study are described and the onset pentad of the SCSSM for each of the years 1955–2001 is defined on the basis of the 850-hPa zonal winds. Relationships among upper-ocean heat content (OHC), ENSO, and SCSSM onset are examined in Section 3. A physical mechanism is then proposed in Section 4 to explain the impact of the ENSO cycle on the SCSSM onset variation. The conclusion and discussion are presented in Section 5.

2. DATA AND DEFINITION

2.1. Data

The data used in this study are mainly from the US National Centers for Environmental Prediction (NCEP) reanalysis and the ECMWF (European Center for Medium-Range Weather Forecasts) 40-year reanalysis (ERA-40). These include the daily and monthly mean values of zonal wind at the 850 and 200 hPa from 1955 to 2001. Daily data of the outgoing longwave radiation (OLR) from the US National Oceanic and Atmospheric Administration for 25 years from 1975 to 2001 (except 1978) are also used. The horizontal resolution of these data is 2.5°latitude/longitude square. For studying the interannual variability, the monthly Niño 3.4 SST anomalies (5°S–5°N, 170–120°W) for 47 years from 1955 to 2001 from the US Climate Prediction Center are employed to identify the warm and cold ENSO years. The monthly gyre-scale upper-ocean temperature (0/400 m) during January 1955 to December 2001 are obtained from http://jedac.ucsd.edu/DATA_IMAGES/, with a global grid resolution of 5°longitude by 2°latitude from 60°N to 60°S. Standard depths include 0, 20, 40, 60, 80, 120, 160, 200, 240, 300, 400 m. Details of this data set can be found in White (1995).

2.2. Monsoon onset date

Some meteorological parameters such as precipitation, prevailing wind, OLR, and cloud-top temperature have been used to define the monsoon onset (Tao and Chen, 1987; Matsumoto, 1989; Xie *et al*., 1998; Lu and Chan, 1999). Wang *et al*. (2004) suggested a wind index – the 850-hPa zonal winds averaged over the region 5°–15°N, 110°–120°E (the precise domain is 3.75°–16.25°N, 108.75°–121.25°E) – to quantify changes in the SCS circulation before, during, and after the onset. The OLR data are used as a proxy for deep convection because of its strong relationship with tropical rainfall (Wu and Zhang, 1998), which is a direct reflection of the summer monsoon. Quite a few studies have used OLR values to define the onset and development of the summer monsoon (e.g., Wu and Zhang, 1998; Xu and Chan, 2001). On the other hand, some authors (e.g., Wang and Wu, 1997) preferred to use both the 850-hPa zonal wind and OLR.

Because OLR data are only available from 1975, the onset dates of the years before 1975 cannot be defined using the OLR. In order to extend the number of years that can be studied, it is necessary to find another index with a longer record, the value of which can give an onset pentad consistent with that from the OLR data. A good candidate is the 850-hPa zonal winds over the central and southern part of the SCS (110–120°E, 5–15°N), which reflects the migration of the subtropical high in and out of the SCS. The onset pentad is therefore defined as the first pentad after mid-April when the 5-day mean value of the 850-hPa zonal winds is westerly over the central and southern part of SCS and lasts for more than two pentads. We also used the ERA-40 data to verify the onset dates defined by the NCEP data and found that the average onset pentad from both time series is the same, being the fourth pentad of May (28th pentad), and only 3 (1971, 1974, 1982) out of 44 (1958–2001) years are different (Appendix 1). The NCEP and ECMWF data therefore give essentially the same SCSSM onset dates. In the following discussion, the NCEP data are used. An early or late MOD is classified using pentad 28 (P28, the mean onset pentad of MOD) as the threshold, with the 47 years being stratified into three groups (Table I): 14 extremely early (E < P27), 23 normal, and 10 extremely late (L > P29). The 23 normal cases can be further subdivided into 7 early to normal onset (NE = P27) cases, 7 normal onset (N = P28) cases, and 9 late to normal onset (NL = P29) cases. The reason for the fine division within the normal category will become apparent in the following sections.

2.3. Ocean heat content

Because of the deep ocean mixed layer and the extensive warm pool over the tropical WNP, the horizontal and vertical gradients of sea-surface temperature (SST) and its temporal changes tend to be small. On the other hand, subsurface water temperature changes are driven by wind

Table I. Classification of MOD. EE, NE, NN, NL, and EL represent extreme early onset (<27 pentad), early to normal onset (=27 pentad), normal onset (=28 pentad), late to normal onset (=29 pentad), and extreme late onset (>29 pentad).

EE	<P27	1956, 1960, 1966, 1971, 1972, 1974, 1976, 1984, 1985, 1994, 1996, 1999, 2000, 2001
NE	=P27	1957, 1961, 1979, 1980, 1981, 1986, 1995
NN	=P28	1962, 1964, 1977, 1989, 1990, 1992, 1997
NL	=P29	1955, 1958, 1965, 1967, 1969, 1978, 1983, 1988, 1998
EL	>P29	1959, 1963,1968, 1970, 1973, 1975, 1982, 1987, 1991, 1993

DOI: 10.1002/joc

stresses. ENSO signal in the wind stresses affects the vertical extent of the thermocline, so that the strongest ENSO signal occurs in the subsurface (Wang *et al*., 1999). From the ocean dynamics point of view, the thermocline depth could be roughly represented by the 20 °C isotherm within the thermocline layer (Kessler, 1990). To estimate the depth of this isotherm, the mixed-layer ocean temperature (0/400 m) data are interpolated to 1×1 m vertical resolution using cubic splines, and the OHC above the thermocline could then be integrated as

$$Q = S \int_{-h}^{0} \rho \, C_{\mathrm{p}} T \, \mathrm{d}z$$

where S stands for unit grid area, C_{p} the specific heat capacity at constant pressure, ρ the density of the fluid, h the depth of a 'representative' isotherm (20 °C), and T the temperature of the mixed layer.

3. INTERANNUAL VARIABILITIES OF MOD AND OHC

3.1. Relationship between OHC, ENSO, and MOD

Kinter *et al*. (2002) stated that the most fundamental and important oceanic indicators for ENSO are SST and OHC. Previous studies have also suggested that the movements of upper-ocean warm water in the Pacific and ENSO events are closely related (Wyrtki, 1985; Zebiak, 1989; Springer *et al*., 1990). The correlation coefficient between Niño3.4 SST and the OHC at each grid point (Figure 1) exhibits two distinct 'dipole' patterns: the Indian dipole and the Pacific dipole, with negative (positive) correlations over the eastern (western) Indian Ocean and western (eastern) Pacific Ocean. Note that the values of the correlation coefficient in the Indian Ocean are relatively smaller compared with those in the Pacific Ocean, which suggests that variations of the OHC anomalies in the Pacific Ocean should be more related to ENSO. These results agree well with the idea that accumulation of warm water in the western (eastern) Pacific warm pool is associated with an EN (La Niña) onset (Wyrtki, 1985). It is interesting to note from Figure 1 that the positive (negative) centers over both the Pacific and Indian oceans are south (north) of the equator, and the dateline (90°E) becomes the line separating positive and negative correlations in the Pacific (Indian) Ocean. Though significant at 95% confidence level, the Indian dipole is less prominent than the Pacific dipole. Therefore, the rest of the paper will focus on the variations of OHC anomalies in the western and eastern equatorial Pacific (EEP), and their impact on the corresponding MOD variations.

The anomalies over the Pacific can be combined by defining a Pacific dipole index (PDI) as the OHC difference averaged over each box in Figure 1 [western (130–170°E, 0–10°N) minus eastern (110–150°W, 6°S–4°N)]. The time series of PDI show large negative (positive) values at the ENSO cold (warm) phase (Figure 2), with a correlation of −0.87 with Niño3.4 SST. That is, during an EN event, an OHC discharge (charge) occurs over the western (eastern) equatorial Pacific so that PDI is negative. The reverse occurs during a La Niña event.

Another important feature in Figure 2 is that the variation of MOD (Table I) generally follows the trend of the PDI. That is, the MOD tends to be earlier (later) when the PDI is positive (negative). In other words, the OHC dipole patterns might be related to the timing of the SCSSM onset, with charged (discharged) OHC anomalies over the western Pacific warm pool and discharged (charged) OHC anomalies over the EEP associated with an early (late) SCSSM onset.

3.2. ENSO cycles associated with OHC and MOD

Li and Mu (1999) suggested that an eastward propagation of positive anomalies of subsurface ocean temperature (SOT) in the Pacific warm pool region is the main reason for the EN occurrence. They further pointed out that the ENSO cycle results from the SOT anomaly cycle in the tropical Pacific (Li and Mu, 2002). The longitude–time sections of OHC composites along the equator show that, for the early onset cases (Figure 3(a)), in year

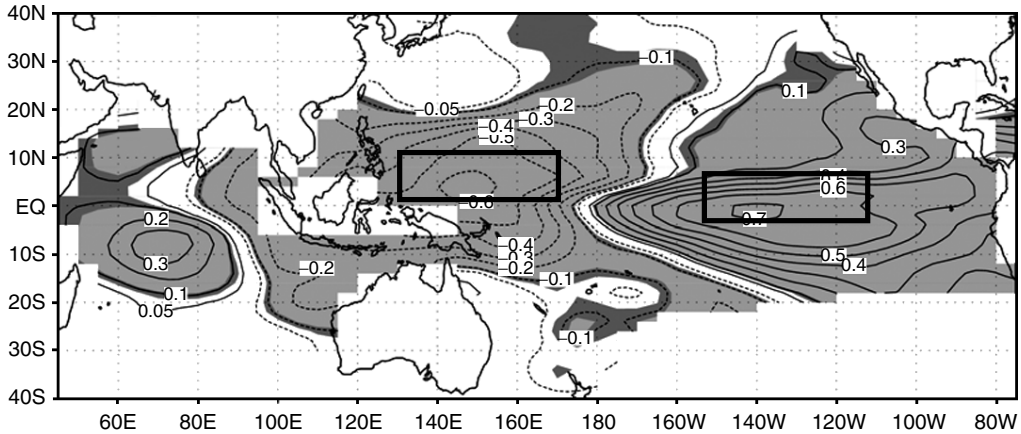

Figure 1. Simultaneous correlation between monthly Niño3.4 SST and OHC field (1955–2001). Shaded areas indicate correlation coefficients significant at the 95% (dark gray) and 99% (light gray) confidence level.

DOI: 10.1002/joc

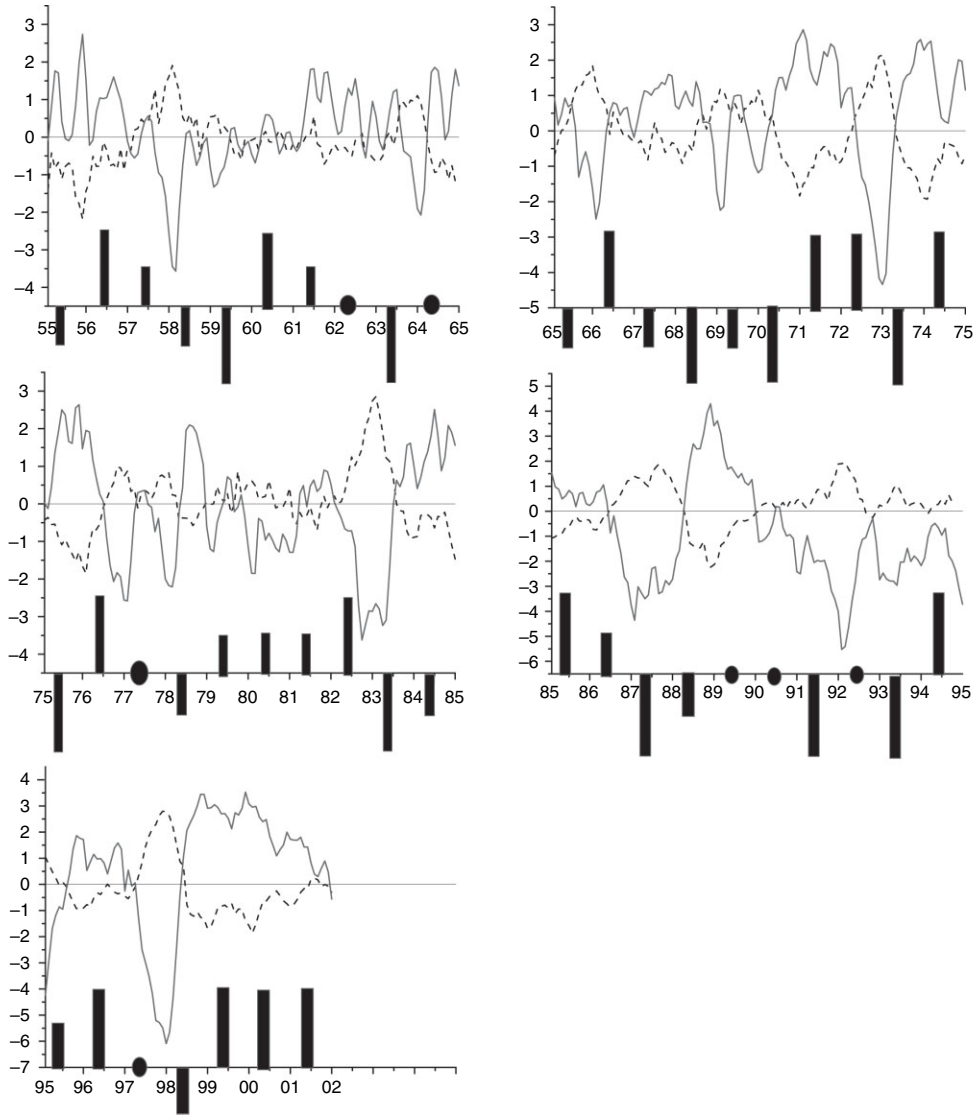

Figure 2. Normalized monthly Pacific dipole index [OHC averaged over western Pacific (130–170°E, 0–10°N) minus OHC averaged over eastern Pacific (150–110°W, 6°S–4°N)] (solid) and Niño3.4 index (dashed). Long bars above (below) the abscissa indicate early (late) onset, short bars above (below) the abscissa indicate normal to early onset (normal to late onset), dot along the abscissa indicate normal onset.

−2 positive (negative) OHC anomalies exist over the eastern (western) equatorial Pacific, which is typical of the mature phase of an EN event. (Year 0 is defined as the year in which the MOD of a particular type is considered. Year ($-n$) refers to n year(s) before, and year (n) to n year(s) after, year 0.) The negative OHC anomalies then propagate eastward and reach the central equatorial Pacific (CEP) by the winter of year −1 (Dec, −1 to Feb, 0), signifying the mature stage of La Niña (LN). At this time, OHC anomalies over the western equatorial Pacific (WEP) have become positive. These positive anomalies begin to propagate eastward towards the end of year 0. These results suggest that early onset cases in year 0 mostly occur from an EN type in year −2 or −1 to the LN type in year 0. Almost the exact reverse occurs for the late onset cases (Figure 3(b)), although the eastward propagation of the positive OHC anomalies is not as strong. In fact, the maximum positive OHC anomalies appear to remain in the CEP during the winter of year −2 and year −1. Nevertheless, it is apparent that these late MOD cases are associated with an EN type that follows from an LN type.

This conclusion is further substantiated by the fact that 11 out of 14 early onset cases occurred either during an LN year or the year after an LN event (LN + 1) (Table II), and 8 out of 10 late onset cases are associated with either an EN event or the year after an EN event (EN + 1). These results suggest that the SCSSM onset date may be tuned to the ENSO cycle, with late and early onsets taking turns. In other words, variations of MOD appear to follow the ENSO cycle (Figure 2). For example, from an LN event to an EN event, the SCSSM experiences an NE (normal to early) or E (early) onset and then an NL (normal to late) or L (late) onset, e.g. 1956–1958, 1971–1973, 1974–1978, 1985–1987, and 1995–1998. Likewise, from an EN event to an LN event, the onset time sequence reverses, e.g. 1968–1971, 1983–1985, 1987–1989, 1991–1996, and 1997–2001.

DOI: 10.1002/joc

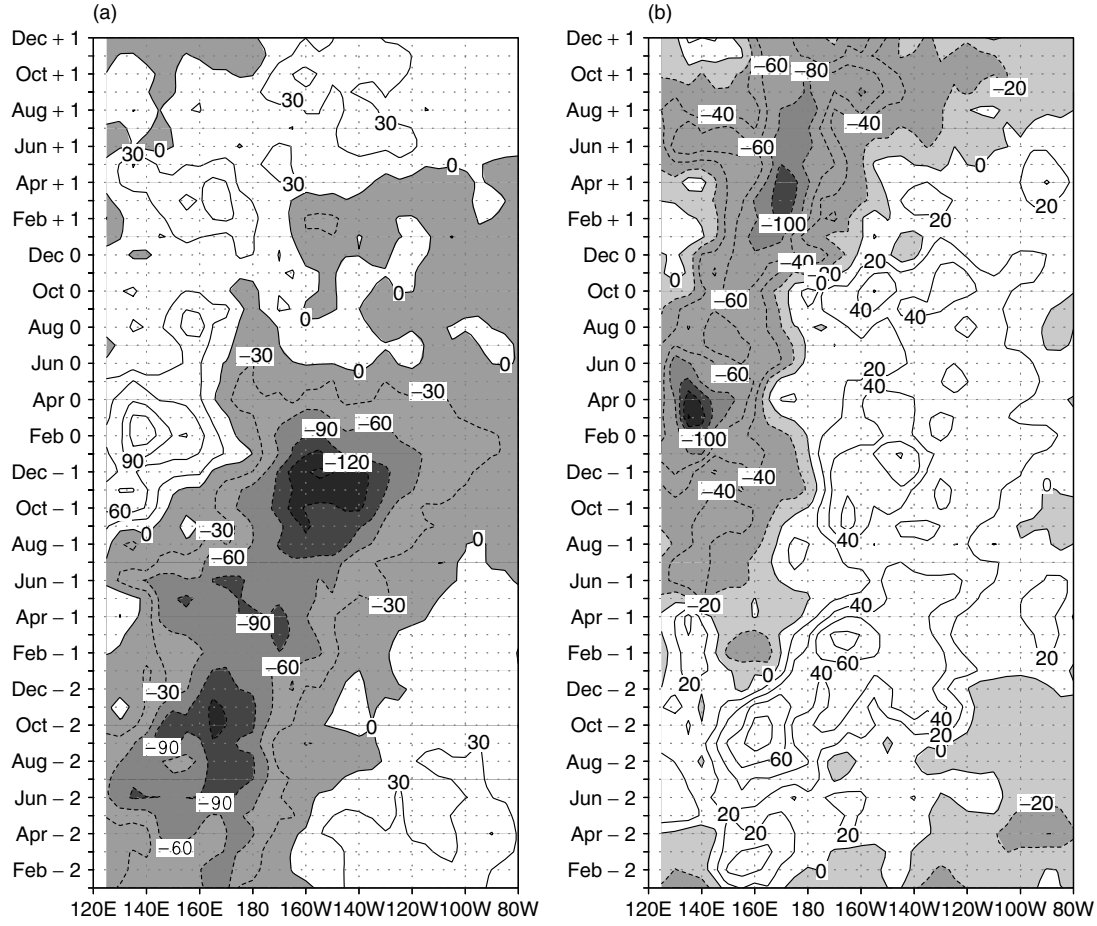

Figure 3. Longitude–time section of OHC anomaly composites (unit: 10^8 J m^{-2}) averaged over 4°S–4°N for (a) E onset years and (b) L onset years. Year 0, +1, and −1 (−2) refer to the monsoon onset year, the year after, and the year (two years) before. Shaded areas indicate negative values.

Table II. ENSO event and MOD. LN, LN + 1, EN, EN + 1, and *neutral* refer to the La Niña year, the year after a La Niña, the El Niño year, the year after an El Niño, and non-ENSO year, respectively. Parentheses indicate the year LN + 1/EN or EN + 1/LN.

	Early onset (14 cases)	Late onset (10 cases)
LN/LN + 1	1956, 1971, (1972), 1974, 1976, 1984, 1985, 1996, 1999, 2000, 2001	1975
EN/EN + 1	1966, 1994	1963, 1968, (1970), (1973) 1983, 1987, 1991, 1993
Neutral	1960	1959

It is also interesting to note from Figure 3(b) that warm water propagates eastward as fast, warm Kelvin waves, but cold water (Figure 3(a)) moves eastward as slow, cold Kelvin waves. The OHC evolution in Figure 3 indicates that cold (warm) Kelvin wave moving eastward occurs during winter to spring (summer to autumn). The reason why the occurrence timing is different is an issue for future work.

If the monthly mean magnitude of the 850-hPa zonal winds averaged over the central and southern parts of the SCS (110–120°E, 5–15°N) is used as a proxy for the intensity of the SCSSM, similar variations in the SCSSM intensity can also be observed (Figure 4). For E onset years, the SCSSM appears to be weak in both year −2 and year −1, but strong in year 0 and year 1. The reverse occurs for the L onset years. This result suggests that the adjustment cycle of SCSSM from strong to weak is generally related to the MOD cycle from early onset to late onset, and vice versa.

4. POSSIBLE MECHANISM

The results in Section 3.2 suggest an apparent 4-year oscillation, which can actually be identified from a MTM (Multi-taper Method) spectrum analysis (Figure 5). As is expected, a prominent harmonic cycle of around 4–5 year stands out clearly from the white noise at

DOI: 10.1002/joc

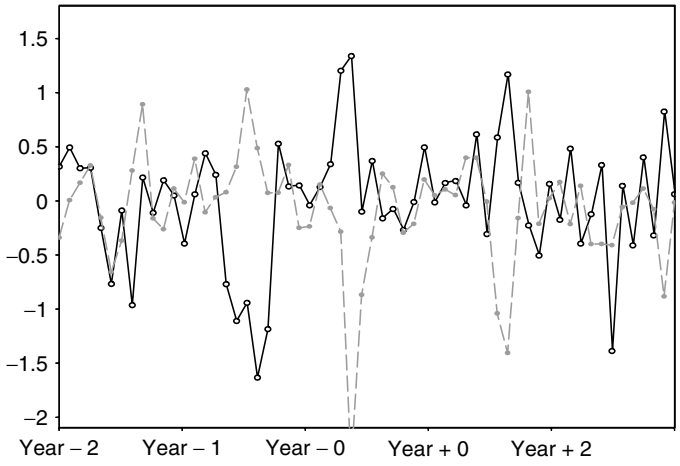

Figure 4. The 4-year variation of 850-hPa zonal wind anomalies (unit: m s^{-1}) over the southern part of SCS (110–120°E, 5–15°N) for E onset years (solid line) and L onset years (dashed line). Year 0, +1, and −1 (−2) refer to the monsoon onset year, the year after, and the year (2 years) before.

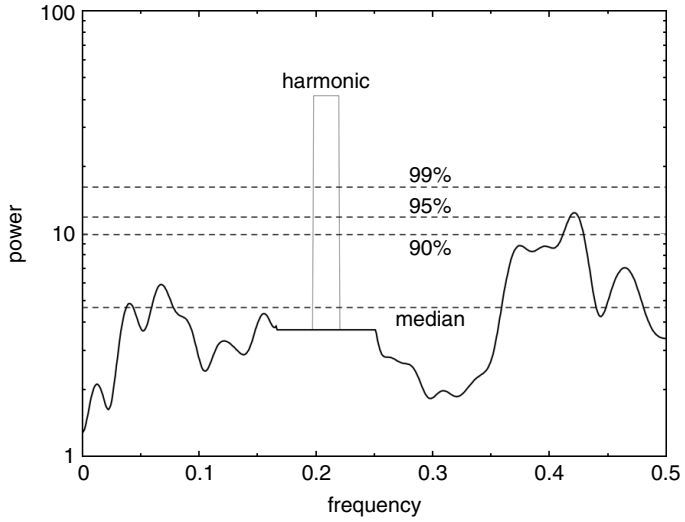

Figure 5. MTM spectrum of the MOD time series. The four smooth dashed lines, from bottom to top, indicate the median, 90, 95, and 99% significance levels.

the 99% significance level. A second peak can also be observed in the 2–3 year band if the 95% significance level is used as the cut-off. In this section, we will attempt to provide a physical explanation for this apparent 4-year oscillation, which is likely related to the evolution of ENSO.

4.1. Correlations with OHC

To investigate the relationship between MOD and ENSO (as represented by the OHC distribution), the MOD is correlated with the three-month-averaged values of the OHC over the entire Pacific from 2 years before the onset to the months of the onset. Positive correlations are found in the WEP starting from January–March (JFM) of year −2 (Figure 6). A positive correlation means that the SSTA in these three months is negative (positive) for an early (late) onset in year 0. At the same time, significant negative correlations are found in the EEP. The positive correlation over the WEP becomes significant in the April–June (AMJ) of year −2, and increases in July–September (JAS) of year −2, and then propagates eastward obviously in October–December (OND) of year −2. By JFM of year −1, the positive correlation has reached the CEP while the negative correlation over the EEP in the year −2 has disappeared. By JAS of year −1, an area of significant negative correlation appears in the WNP at around 10°N. The center of this area propagates westward while that of the area of positive correlation continues to propagate eastward, reaching the coast of South America by JFM of year 0. The center of the negative correlation area now reaches just east of the Philippine Sea. By the onset of the summer monsoon, both the positive and negative correlations have decreased.

4.2. The physical mechanism

A cross wavelet and wavelet coherence analysis (Grinsted *et al*., 2004) further supports the cyclic relationship

DOI: 10.1002/joc

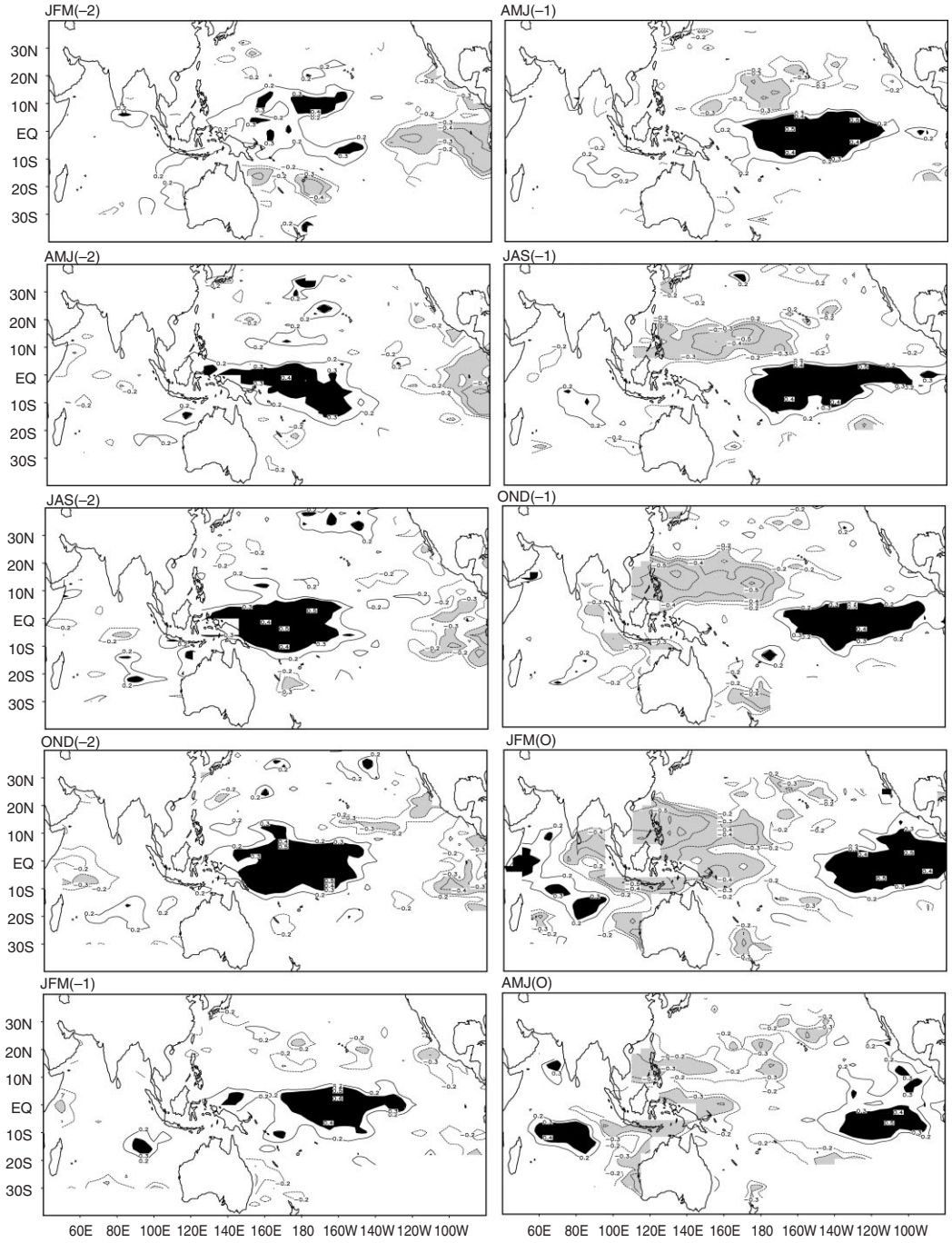

Figure 6. Correlation between MOD and OHC for the period 1955–2001. Year 0 refers to the monsoon onset year, year −1 (−2) refers to the year (2 years) before the monsoon onset year. JFM, AMJ, JAS, and OND indicate the 3-month averages for January–February–March, April–May–June, July–August–September, and October–November–December.

between ENSO and SCSSM onset. The cross wavelet analysis (Figure 7(a)) reveals areas with high common power of both PDI and MOD. Within the significant sectors, they are in antiphase (in the 2–3 year band during 1972–1977, in the 4–5 year band during 1980–1995). As PDI has a negative correlation (−0.87) with Niño3.4 SST, ENSO and MOD are likely to be in phase within the 2–7 year period. An interdecadal variation might also exist.

The wavelet coherence is another useful tool to measure how coherent the cross wavelet transformations of PDI and MOD are in frequency space. Compared with Figure 7(a), a larger significant section is found (Figure 7(b)), again with antiphase behavior between PDI and MOD, especially at periods of ∼4 years. Almost all the significant sectors are around post-1976. The oscillations of the MOD are manifested in the PDI at periods varying from 2–7 years and 12–15 years.

All these results are consistent with one another in terms of the ENSO evolution. A possible mechanism for the interannual variation of the onset date of the SCSSM could be as follows.

DOI: 10.1002/joc

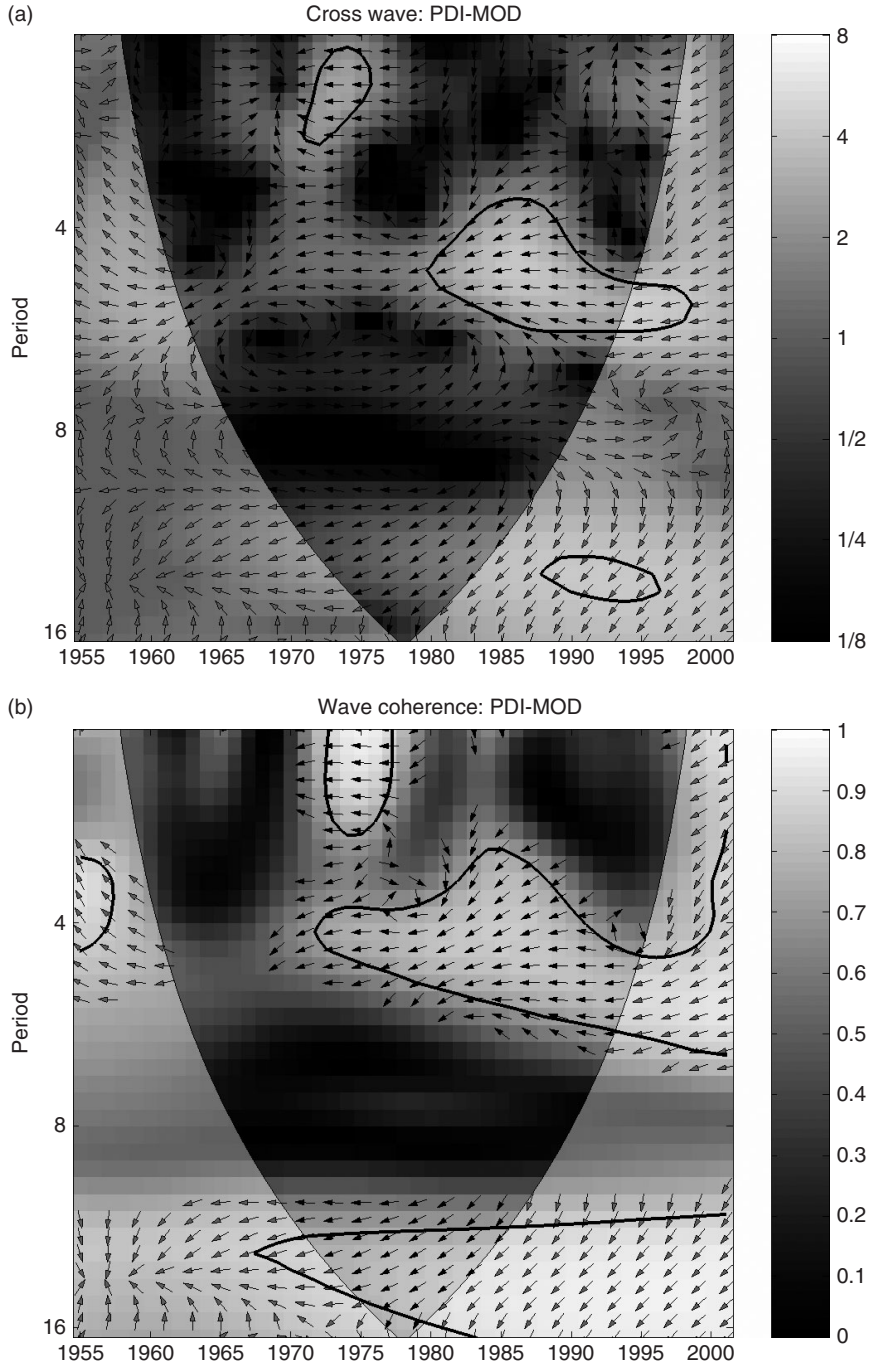

Figure 7. Cross wavelet transform (a) and squared wavelet coherence (b) between the standardized PDI and MOD time series. Thick contour indicates the 5% significance level against red noise. Arrows suggest the relative phase relationship, with those in phase pointing right and those not in phase pointing left, and PDI leading MOD by 90° pointing straight down.

Consider a late monsoon onset case in year 0. Two years before (year −2), the onset is likely to be normal or early (Figure 4). In other words, the circulation anomaly over the Philippine Sea is likely to be cyclonic. This is then related to a pre-EN onset situation so that warm subsurface water over the WEP propagates eastward while subsurface water over the EEP tends to be cold (hence the correlation patterns in Figure 6). As the warm subsurface water continues to move eastward as Kelvin waves, the cold water is displaced poleward, so that the negative correlation along the South American coast decreases. The cold water then propagates westward as a Rossby-wave response. When the cold water reaches the WNP, it weakens the warm pool and hence intensifies the subtropical high. The strengthening of the subtropical high leads to an enhancement of the easterlies and hence stronger upwelling and cold subsurface water (JFM, year 0, Figure 3). Persistence of the strengthening of the subtropical high also results in its westward extension and hence a weak winter monsoon (the case for EN + 1; Li and Mu, 2002) and then a late summer monsoon onset (year 0, EN + 1).

DOI: 10.1002/joc

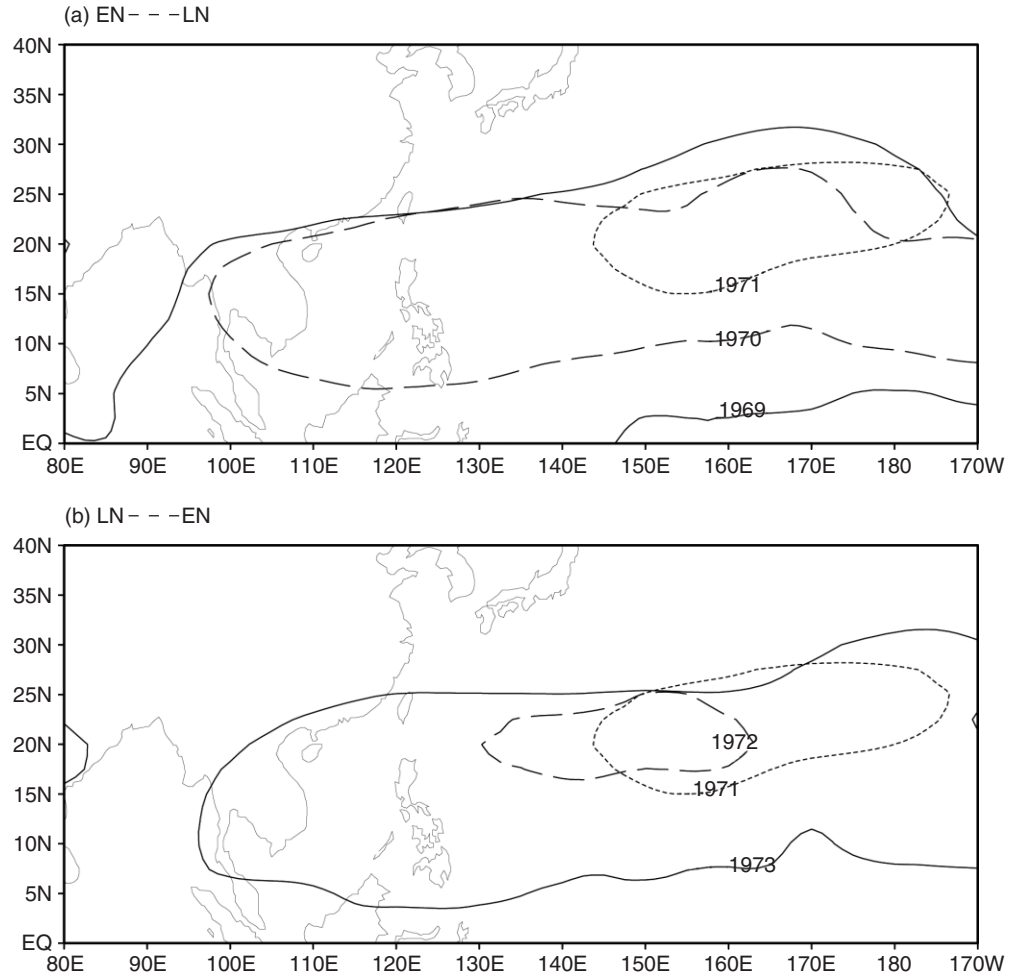

Figure 8. The monthly 500-hPa geopotential height, indicated by the 5860-m contour, for (a) from EN year to LN year: May of 1969 (solid), 1970 (long-dashed), and 1971 (short-dashed); and (b) from LN year to EN year: May of 1971 (short-dashed), 1972 (long-dashed), and 1973 (solid).

A persistent subtropical high results in an increase in insolation, which will subsequently lead to an increase in SST. This would weaken the subtropical high, or the development of cyclonic anomalies. The other half of the cycle then repeats.

An example of this entire cycle is shown for the period of 1969–1973. From EN to LN year (Figure 8(a)), the subtropical high goes from strong (1969 and 1970) to weak (1971). Then, from LN year to EN year (Figure 8(b)), the subtropical ridge goes from weak (1971, 1972) to strong (1973). This cycle is then associated with the SCSSM onset cycle of NL (1969) → L (1970) → E (1971, 1972) → L (1973). Similar cycles have been observed in other years in which EN to LN and then back to EN situations occurred.

5. SUMMARY AND DISCUSSION

5.1. Summary

This paper examines the interannual variability of the onset date of the SCSSM and its relationship with the ENSO. The MOD is defined on the basis of switching the 850-hPa zonal winds over the SCS from easterly to westerly for two consecutive pentads. The ENSO signal is represented by the OHC, which is proportional to the depth of the 20 °C isotherm.

It is found that, for years associated with a warm (cold) ENSO event or the year after, the monsoon tends to have a late (an early) onset and the intensity of the SCSSM also tends to be weaker (stronger). During a 2-year period prior to the onset, anomalies of OHC have an obvious eastward propagation. An examination of the low-level circulation suggests that the 850-hPa flow east of the Philippines, specifically the strength of the subtropical high, is critical in determining the MOD. This appears to be related to the propagation of the subsurface water both eastward along the Equator and westward in the North Pacific. Propagation of cold (warm) water into the WNP apparently strengthens (weakens) the subtropical high, which results in a late (an early) SCSSM onset.

5.2. Discussion

OHC indeed reflects the ENSO evolution. It not only 'memorizes' the effects of SST on winds, but also conveys the feedback of the winds to SST later on.

DOI: 10.1002/joc

Wang *et al*. (1999) suggested that the ENSO transition from a warm (cold) phase to a cold (warm) phase might be triggered by the anomalous anticyclonic (cyclonic) wind stress curl developed *in situ* over the WNP. The anomalous anticyclonic wind stress curl helps discharge the OHC in the WNP warm pool by inducing *in situ* Ekman downwelling and thermocline deepening. The anomalous easterlies to the south of the anticyclone could raise the thermocline, propagate the elevated thermocline along the equator, and lead to the decay of the equatorial eastern Pacific warming, which have been discussed in detail in Wang *et al*. (1999). The present study further suggests that ENSO, through its modification of the strength of the subtropical high in the WNP, is one of the factors determining the time of onset and the intensity of the SCSSM. The lower-level zonal wind in the tropics provides the dynamic conditions for ENSO events. During the mature phase of LN events, the development of cyclonic circulation in the low-level tropical western pacific causes the westerly wind anomaly over Indonesia and the tropical western Pacific. When EN develops into its mature stage, an anticyclonic circulation anomaly in the tropical western Pacific causes easterly wind anomalies in Indonesia and the equatorial western Pacific.

While an apparent 4-year cycle is present, this should be interpreted with caution, mainly because the ENSO cycle itself is not periodic. Other factors must also be taken into consideration if a prediction is to be made. It can be noted that the cycle of the onset time of the SCS summer monsoon not only originates from the air–sea interaction in the tropical Pacific, but also from that in the Indian Ocean – an antiphase behavior over Indian Ocean shown in Figure 6 from year −2 to year 0 stands out. To some extent, there is a lack of a physical mechanism to interpret such a strong linkage between the time of onset, early/late cycle, and the ENSO cycle, and further simulations about this relationship will have to be tested. Nevertheless, the results do provide some useful information for such predictions.

ACKNOWLEDGEMENTS

The authors would like to thank the US NCEP for providing the monthly global reanalysis data (1958–2000), the National Oceanic and Atmospheric Administration for the OLR data (1975–2000), the Scripps Institution of Oceanography for the monthly mixed-layer ocean temperature (0/400 m), Y. Liu of the South China Sea Institute of Oceanology, Chinese Academy of Sciences and A. Grinsted of the Arctic Center of the University of Lapland in Finland for the OHC calculation method and cross wavelet/wavelet coherence method, respectively.

This research is partially supported by the City University of Hong Kong Research Grant No. 7001682.

Appendix I

The onset pentad defined by the ERA40/NCEP 850-hPa zonal wind over SCS (110–120°E, 5–15°N). Bold numbers indicate that the two onset pentads are different

Year	NCEP	ECMWF
1958	29	29
1959	30	30
1960	30	30
1961	27	27
1962	28	28
1963	30	30
1964	28	28
1965	29	29
1966	25	25
1967	29	29
1968	30	30
1969	29	29
1970	32	31
1971	**25**	**26**
1972	26	26.
1973	33	33
1974	**26**	**24**
1975	23	23
1976	26	26
1977	28	28
1978	29	29
1979	27	27
1980	27	27
1981	27	27
1982	**31**	**25**
1983	29	29
1984	24	24
1985	23	23
1986	27	27
1987	32	32
1988	29	29
1989	28	28
1990	28	28
1991	32	32
1992	28	28
1993	32	32
1994	25	25
1995	27	27
1996	26	26
1997	28	28
1998	29	29
1999	23	23
2000	26	26
2001	26	26

REFERENCES

Angell JK. 1981. Comparison of variations in atmospheric quantities with sea surface variations in the equatorial eastern Pacific. *Monthly Weather Review* **109**: 230–243.

Chang C-P, Zhang YS, Li T. 2000. Interannual and Interdecadal variations of the east Asian summer monsoon and tropical Pacific SSTs. Part II: Meridional structure of the monsoon. *Journal of Climate* **13**: 4326–4340.

Grinsted A, Moore JC, Jevrejeva S. 2004. Application of the cross wavelet transform and wavelet coherence to geophysical time series. *Nonlinear Processes in Geophysics* **11**: 561–566.

DOI: 10.1002/joc

Huang RH, Sun F. 1992. Impacts of the tropical western Pacific on the East Asian summer monsoon. *Journal of the Meteorological Society of Japan* **70**: 243–256.
Ju J, Slingo J. 1995. The Asian summer monsoon and ENSO. *Quarterly Journal of the Royal Meteorological Society* **121**: 1133–1168.
Kessler WS. 1990. Observations of long Rossby waves in the northern tropical Pacific. *Journal of Geophysical Research* **95**: 5183–5217.
Kinter JL, Miyakoda K, Yang S. 2002. Recent change in the connection from the Asian monsoon to ENSO. *Journal of Climate* **15**: 1203–1215.
Lau K-M, Yang S. 1997. Climatology and Interannual variability of the Southeast Asian summer monsoon. *Advances in Atmospheric Sciences* **14**: 141–162.
Li C, Mu M. 1999. El Niño occurrence and sub-surface ocean temperature anomalies in the Pacific warm pool. *Chinese Journal of the Atmospheric Sciences* **5**: 513–521.
Li C, Mu M. 2002. A further study of the essence of ENSO. *Chinese Journal of the Atmospheric Sciences* **4**: 309–328.
Lu E, Chan JCL. 1999. A unified monsoon index for South China. *Journal of Climate* **12**: 2375–2385.
Matsumoto J. 1989. Heavy rainfalls over East Asia. *International Journal of Climatology* **9**: 407–423.
Nitta T, Hu ZZ. 1996. Summer climate variability in China and its association with 500 hPa height and tropical convection. *Journal of the Meteorological Society of Japan* **74**: 425–445.
Oort AH, Yienger JJ. 1996. Observed interannual variability in the Hadley circulation and its connection to ENSO. *Journal of Climate* **9**: 2751–2767.
Rasmusson EM, Carpenter TH. 1983. The relationship between eastern equatorial Pacific sea surface temperatures and rainfall over India and Sri Lanka. *Monthly Weather Review* **111**: 517–528.
So CH, Chan JCL. 1997. An observational study on the onset of the summer monsoon over South China around Hong Kong. *Journal of the Meteorological Society of Japan* **75**: 43–57.
Springer SR, McPhaden MJ, Busalacchi AJ. 1990. Oceanic heat content variability in the tropical Pacific during the 1982–1983 El Nino. *Journal of Geophysical Research* **95**: 22089–22101.
Wang B, Wu R. 1997. Peculiar temporal structure of the South China Sea summer monsoon. *Advances in Atmospheric Sciences* **14**: 177–194.
Wang B, Wu R, Lukas R. 1999. Roles of the western North Pacific wind variation in thermocline adjustment and ENSO phase transition. *Journal of the Meteorological Society of Japan* **77**: 1–16.
Wang B, Wu R, Fu X. 2000a. Pacific–East Asian teleconnection: How does ENSO affect East Asian Climate? *Journal of Climate* **13**: 1517–1536.
Wang B, Wu R, Lukas R. 2000b. Annual adjustment of the thermocline in the tropical Pacific Ocean. *Journal of Climate* **13**: 596–616.
Wang B, LinHo Y, Zhang Y, Lu M-M. 2004. Definition of South China Sea Monsoon onset and commencement the East Asia Summer Monsoon. *Journal of Climate* **17**: 699–710.
Webster PS, Yang S. 1992. Monsoon and ENSO: selectively interactive systems. *Quarterly Journal of the Royal Meteorological Society* **118**: 887–926.
White WB. 1995. Design of a global observing system for gyre-scale upper ocean temperature variability. *Progress in Oceanography* **36**: 169–217, Pergamon.
Wu G, Zhang Y. 1998. Tibetan Plateau forcing and the timing of the monsoon onset over South Asia and the South China Sea. *Monthly Weather Review* **126**: 913–927.
Wyrtki K. 1985. Water displacements in the Pacific and the genesis of El Nino cycles. *Journal of Geophysical Research* **90**: 7129–7132.
Xie A, Chung YS, Liu X, Ye Q. 1998. The interannual variations of the summer monsoon onset over the South China Sea. *Theoretical and Applied Climatology* **59**: 201–213.
Xu J, Chan JCL. 2001. The role of the Asian/Australian monsoon system in the onset time of El Niño events. *Journal of Climate* **14**: 418–433.
Zhang R, Sumi A, Kimoto M. 1996. Impact of El Niño on the East Asian monsoon: A diagnostic study of the '86/87 and '91/92 events. *Journal of the Meteorological Society of Japan* **74**: 49–62.
Zebiak SE. 1989. Oceanic heat content variability and El Nino cycles. *Journal of Physical Oceanography* **19**: 475–486.

DOI: 10.1002/joc